Hydrophobin-functionalized film bulk acoustic wave resonators for sensitive and polarity-sensitive sensing of volatile organic compounds

Article *in* Applied Physics Letters · October 2019

DOI: 10.1063/1.5124525

CITATIONS
0

READS
91

7 authors, including:

Jin Tao
Changchun Institute of Optics, Fine Mechanics and Physics
16 PUBLICATIONS **167** CITATIONS
SEE PROFILE

Ye Chang
Tianjin University
28 PUBLICATIONS **206** CITATIONS
SEE PROFILE

Jingqiu Liang
Changchun Institute of Optics, Fine Mechanics and Physics
70 PUBLICATIONS **184** CITATIONS
SEE PROFILE

Xuexin Duan
Tianjin University
153 PUBLICATIONS **1,272** CITATIONS
SEE PROFILE

Applied Physics Letters

Hydrophobin-functionalized film bulk acoustic wave resonators for sensitive and polarity-sensitive sensing of volatile organic compounds

Cite as: Appl. Phys. Lett. **115**, 163502 (2019); https://doi.org/10.1063/1.5124525
Submitted: 15 August 2019 . Accepted: 02 October 2019 . Published Online: 14 October 2019

Jin Tao, Ye Chang, Jingqiu Liang, Xuexin Duan, Wei Pang, Yanyan Wang, and Zefang Wang

Applied Physics Letters ARTICLE scitation.org/journal/apl

Hydrophobin-functionalized film bulk acoustic wave resonators for sensitive and polarity-sensitive sensing of volatile organic compounds

Cite as: Appl. Phys. Lett. **115**, 163502 (2019); doi: 10.1063/1.5124525
Submitted: 15 August 2019 · Accepted: 2 October 2019 ·
Published Online: 14 October 2019

Jin Tao,[1,2,3] Ye Chang,[3] Jingqiu Liang,[1] Xuexin Duan,[3] Wei Pang,[3] Yanyan Wang,[3] and Zefang Wang[2,4,a)]

AFFILIATIONS

[1]State Key Laboratory of Applied Optics, Changchun Institute of Optics, Fine Mechanics and Physics, Chinese Academy of Sciences, Changchun 130033, China
[2]College of Life Sciences, Tianjin University, Tianjin 300072, China
[3]State Key Laboratory of Precision Measuring Technology and Instruments, College of Precision Instrument and Opto-electronics Engineering, Tianjin University, Tianjin 300072, China
[4]Tianjin International Joint Academy of Biotechnology and Medicine, Tianjin 300457, China

[a)]**Author to whom correspondence should be addressed:** zefangwang@tju.edu.cn

ABSTRACT

Film bulk acoustic wave resonators have demonstrated great potential in the detection of volatile organic compounds owing to their high sensitivity, miniature size, low power consumption, capacity for integration, and other beneficial characteristics. However, it is necessary to functionalize the surfaces of these resonators to enhance the adsorption and discrimination of volatile organic compounds. Here, we report a convenient and reliable method for functionalizing the surfaces of film bulk acoustic wave resonators with hydrophobins via self-assembly to enable highly sensitive and polarity sensitive detection of volatile organic compounds. Experiments conducted using various concentrations of five volatile organic compounds possessing different polarities demonstrated that the hydrophobin coating enhanced the responsivity of the proposed sensor. The obtained results were in good agreement with the Brunauer–Emmett–Teller model of multilayer physisorption, which suggests that the hydrophobin coating enhanced the sensitivity by improving the monolayer adsorption capacity. Our work demonstrates that the combination of multifunctional biosurfactants and microelectromechanical devices can permit high-performance gas sensing.

The detection of volatile organic compounds (VOCs) is of great significance in the fields of human healthcare, indoor air quality, industrial gas pollution, and forensic science because VOCs are biomarkers of various diseases and disorders[1,2] and among the most important substances known to degrade indoor air quality.[3] VOCs can also be used to determine the causes of crimes[4] and track airborne contaminants.[5] Traditional technologies for detecting VOCs are based on gas chromatography–mass spectrometry and gas chromatography–flame ionization detection.[6,7] However, spectrometer-based VOC-sensing systems are generally expensive and suffer from the lack of portability and high power demand. Optofluidic microsystems are a newly developed analytical technology integrating photonics and microfluidics that possess numerous unique characteristics for enhancing the sensing performance for VOCs.[8–10] Optofluidic VOC detection systems are typically complex because they have to include light sources, photodetectors, pumps, and gas channels. Therefore, it is necessary to develop miniature, portable, inexpensive, and accurate VOC sensors. To date, various small, inexpensive, and fast VOC sensors have been developed, such as chemoresistors,[11,12] metal oxide semiconductor sensors,[13] thermal sensors, hybrid nanostructure sensors,[14,15] mechanical resonator sensors,[16] and optical sensors.[17] Among these methods, resonator sensors are most competitive in terms of sensitivity and resolution owing to the high quality factor of electromechanical resonators.[16]

Film bulk acoustic wave resonators (FBARs), as piezoelectric transducers operating in the gigahertz regime, have been exploited for VOC detection based on the mass loading effect[18–25] and chemical reaction.[26] These sensors feature high sensitivity, miniature size, and low power consumption. FBAR arrays have also been used as electronic noses to achieve discrimination of VOCs.[22–24] A single FBAR can also function as a virtual sensor array with temperature modulation to detect and discriminate VOCs.[25] The surfaces of FBARs are typically functionalized with polymers,[18] supramolecular monolayers,[25] or self-assembled monolayers[23,24] to realize selectivity and improved adsorption. Surface functionalization of the sensors plays a

key role in recognition, sensitivity, selectivity, stability, and reversibility. Polymer coating is the most common surface functionalization method for electronic noses. However, such modification processes are complex and exhibit poor selectivity. In addition, some VOCs can penetrate the polymer bulk, which increases the recovery time and can even cause the sensor to malfunction. Self-assembled monolayers can afford high selectivity and fast adsorption/desorption although the modification process is complex and these monolayers are not robust over prolonged periods.

In our previous work, we demonstrated that hydrophobins are excellent materials for surface functionalization.[27–29] Hydrophobins exhibit remarkable physicochemical properties, such as self-assembly, amphiphilicity, stability, and surface activity.[30–34] Owing to these properties, hydrophobins display a variety of functions at interfaces, including adhesion, formation of coatings, reduction in the surface tension of water, and modification of the hydrophilic/hydrophobic properties of the interfaces. Hydrophobins can also form membranes via self-assembly at air/water or water/solid interfaces.[30] Therefore, hydrophobins hold great potential for applications involving emulsification,[35] separation,[26,27] and interfacial modification.[36–41] It has also been demonstrated that hydrophobins are safe for use in food products[42,43] and exhibit no cytotoxicity, possibly extending their use to personal care and biomedical applications.[14] Moreover, hydrophobins are promising materials for surface modification and as surface membranes in biosensing and electrochemical applications.[44]

In this work, we used HFBI, a hydrophobin from *Trichoderma reesei*,[45,46] to modify the surface of an FBAR and achieve a highly sensitive, stable, and polarity sensitive VOC sensor. HFBI formed a stable and uniform film at the surface of the FBAR via self-assembly. The resulting HFBI film was stable and attractive to polar VOCs. Five VOCs possessing different polarities and concentrations were tested experimentally. Our results were in good agreement with the Brunauer–Emmett–Teller (BET) model of multilayer physisorption, which explains the sensing mechanism of the proposed sensor.

FBARs generally consist of a piezoelectric thin film (e.g., AlN or ZnO) sandwiched between top and bottom electrodes as shown in Fig. 1(a). The detailed fabrication process of FBARs was reported previously.[22] Figure 1(a) presents a cross-sectional view of the FBAR structure coated with an HFBI film layer. Numerous researchers have attempted to exploit FBAR devices for sensor applications with remarkable results.[47] FBAR sensors, which function as mass transducers, are very similar to the well-known quartz crystal microbalance. When a mass (Δm) is added to the device surface, the resonant frequency (f_0) shifts (Δf) as described in the following equation:[47]

$$\Delta f = \frac{2f_0^2}{A\sqrt{\rho\mu}}\Delta m, \tag{1}$$

where A is the surface area of the FBAR and ρ and μ are the density and shear modulus of the piezoelectric material, respectively. The mass sensitivity ($\Delta f/\Delta m$) can be derived from Eq. (1) to be 2.5×10^6 Hz/ng.

The HFBI film was deposited simply by droplet casting. The HFBI solution was prepared by dissolving HFBI (0.50 mg) in phosphate buffer (1 ml, pH 7.2), and 1 μl of this solution was added dropwise onto the surface of the FBAR using a micropipette and allowed to stand for 5 min to undergo self-assembly. Next, the device was washed with pure water and dried under vacuum. Figures 1(b) and 1(c) present images of the bare and HFBI-coated FBARs, respectively.

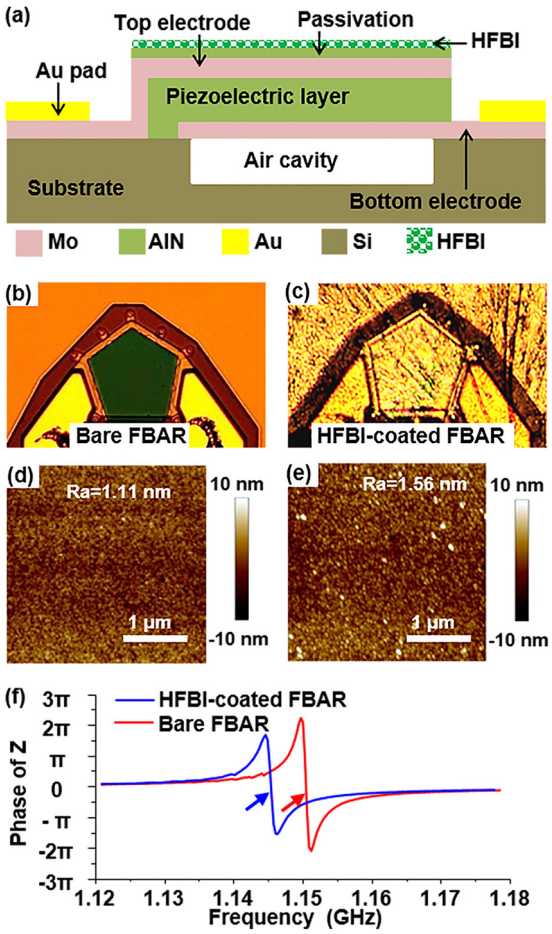

FIG. 1. (a) Cross-sectional view of the FBAR structure coated with an HFBI film layer. Optical microscopy images of a bare FBAR (b) and an HFBI-coated FBAR (c). (d) and (e) AFM images of a bare FBAR and an HFBI-coated FBAR surface. (e) AFM image of the surface. (f) The resonant frequency of the bare FBAR sensor was 1.15272 GHz (red curve). The HFBI coating caused a downward frequency shift of 1.83 MHz (blue curve), corresponding to a mass increase of 0.732 ng.

To check the uniformity of the HFBI film, an atom force microscope was used to measure the smoothness and roughness of the surfaces of the bare FBAR and HFBI-coated FBAR as shown in Figs. 1(d) and 1(e). The surface roughnesses (Ra) of the bare FBAR and HFBI-coated FBAR were found to be 1.11 and 1.56 nm, respectively, indicating that a uniform HFBI film was formed on the FBAR surface.

Figure 1(f) shows the impedance phases of FBAR sensors with (blue curve) and without (red curve) the HFBI coating. The frequency shift was 1.83 MHz, which corresponds to a mass increase of 0.732 ng.

A VOC detection system with two gas channels was established. One channel produced saturated VOC vapor by bubbling pure nitrogen gas (99.999%) through liquid VOCs. The other channel carried pure nitrogen gas to dilute the VOC vapor. The flow velocities were monitored and controlled using a mass flow controller. Various concentrations of VOCs were obtained by adjusting the flow velocity ratio

between the carrier nitrogen and pure nitrogen. The different concentrations of VOCs were quantified as the ratio (P/P_0) of the vapor partial pressure (P) to its saturation vapor pressure (P_0), which was controlled by adjusting the velocities of the two gas channels. The concentration of the VOCs in ppm can be calculated as follows:[48]

$$C(ppm) = 10^6 \times \left(\frac{P_s}{P_t} \times \frac{r}{(r+R)}\right), \quad (2)$$

where P_s is the saturation vapor pressure of the VOC, P_t is the total pressure (760 mm Hg), and r and R are the flow rates (in sccm) of the carrier nitrogen and dilution nitrogen, respectively. Here, $r/(r+R)$ is equal to P/P_0. Further details of the detection system were reported previously.[22,24]

Figures 2(a) and 2(b) present the real-time responses of the bare FBAR and HFBI-coated FBAR sensors upon exposure to seven different concentrations of ethanol vapor. The sensors were first flushed with pure nitrogen to obtain a stable baseline. Next, the FBAR sensors were exposed to ethanol vapor at a constant velocity of 500 sccm. The resulting negative frequency shift indicates the adsorption of ethanol

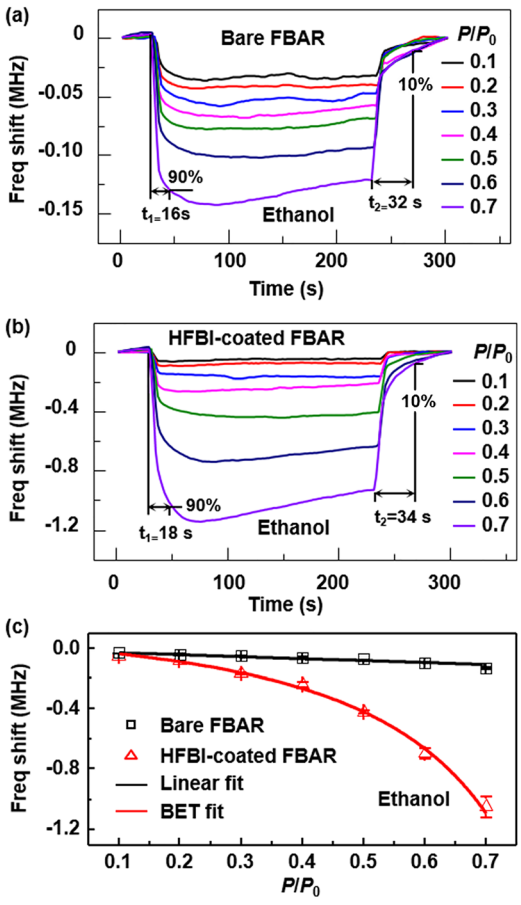

FIG. 2. Real-time responses of the (a) bare and (b) HFBI-coated FBAR sensors to ethanol vapor concentrations (P/P_0) ranging from 0.1 to 0.7, where P and P_0 are the vapor partial pressure and saturation vapor pressure, respectively, at room temperature. (c) Adsorption isotherms for the bare (black) and HFBI-coated (red) FBAR sensors.

molecules to the sensor surface. The response times of the bare FBAR and HFBI-coated FBAR sensors are 16 and 18 s, respectively, for ethanol vapor at a P/P_0 value of 0.7. Next, the vapor flow was switched off, and pure nitrogen was reintroduced to flush the sensor. The frequency recovered back to the baseline in several tens of seconds, indicating that the VOC molecules were removed by the nitrogen gas flow. The recovery times of the bare FBAR and HFBI-coated FBAR sensors are 32 and 34 s, respectively. These results demonstrated that the fabricated sensors exhibited a quick response and full recovery.

To elucidate the adsorption characteristics, adsorption isotherms for the frequency shifts of the two sensors are presented in Fig. 2(c). The black line represents the linear fit of the frequency shift of the bare FBAR sensor upon exposure to ethanol vapor at partial pressures (P/P_0) ranging from 0.1 to 0.7. The adsorption isotherm was almost linear and fitted well with the Langmuir adsorption theorem,[49] indicating the monolayer adsorption of the ethanol molecules at the bare FBAR sensor surface in a concentration-dependent manner owing to weak van der Waals forces between the ethanol molecules and the FBAR sensor surface. The adsorption of the ethanol molecules to the FBAR surface led to a downward shift of the resonant frequency. As van der Waals forces between device surfaces and ethanol molecules are relatively weak, this interaction was concentration dependent and reversible. Upon switching off the ethanol flow and flushing the sensor with nitrogen gas, the resonant frequency of the device recovered to the baseline.

In contrast, the adsorption isotherm for the HFBI-coated FBAR sensor upon exposure to ethanol vapor [red curve in Fig. 1(c)] was more exponential than linear and was well fitted by the BET model of multilayer physisorption.[24,50] In the BET model, the adsorption of gas molecules at a solid interface is physical and multilayer. The adsorption is dependent on the gas concentration and the attractive force between the gas and solid interface. The BET equation can be expressed as follows:

$$v = \frac{v_{m(P/P_0)C}}{1 + (C-2)(P/P_0) - (C-1)(P/P_0)^2}, \quad (3)$$

where v, v_m, and C are the adsorption capacity, monolayer adsorption capacity, and adsorption energy constant, respectively. The values of v_m and C are typically dependent on the nature of the solid surface and gas, allowing them to be used as "fingerprints" for the detection and discrimination of VOCs.

The HFBI coating improved the sensitivity to ethanol by eightfold at a P/P_0 value of 0.7. The most plausible explanation for this is that HFBI is more attractive to ethanol molecules than the bare FBAR surface (AlN) owing to the negatively charged nature of HFBI. As ethanol molecules are also highly polar, the sensitivity enhancement upon HFBI coating can be attributed to polarity. To confirm this hypothesis, hexane, a nonpolar VOC, was also investigated as shown in Fig. 3.

The response times of the bare FBAR and HFBI-coated FBAR sensors are 9 and 13 s, respectively, for hexane vapor at a P/P_0 value of 0.7. The recovery times of the bare FBAR and the HFBI-coated FBAR sensors are 9 and 22 s, respectively. Figure 3(c) shows the adsorption isotherms for the bare (black data points and fitting line) and HFBI-coated (red data points and fitting line) FBAR sensors upon exposure to hexane vapor. Although the HFBI coating improved the sensitivity toward hexane by approximately twofold, this improvement was smaller than that

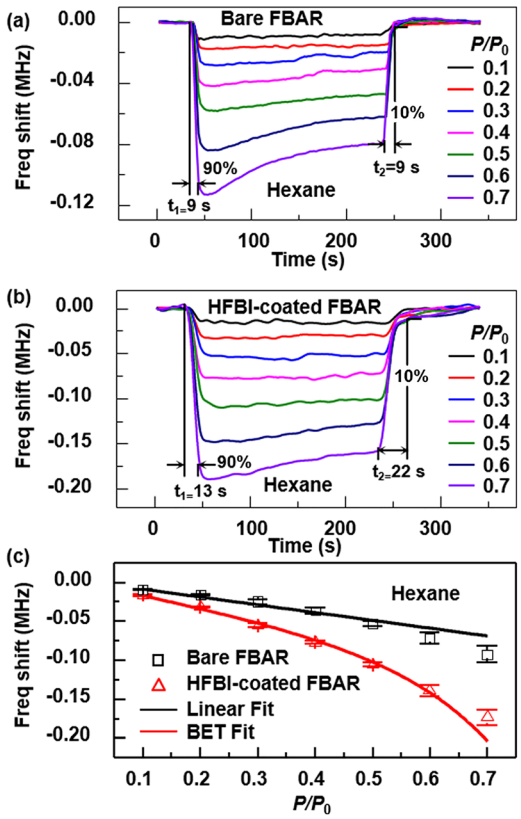

FIG. 3. (a) Real-time responses of the (a) bare and (b) HFBI-coated FBAR sensors to hexane vapor concentrations (P/P_0) ranging from 0.1 to 0.7. (c) Adsorption isotherms for the bare (black) and HFBI-coated (red) FBAR sensors.

observed for ethanol because hexane molecules are nonpolar, leading to weaker attractive forces between the hexane molecules and HFBI.

To further evaluate the amplification effect of the HFBI coating, three additional VOCs (methanol, tetrahydrofuran, and acetone) were tested. Figure 4(a) compares the observed frequency shifts for various concentrations of the five VOCs possessing different polarities. Here, we define the amplification factor as the ratio of the frequency shift for the HFBI-coated FBAR sensor to that for the bare FBAR sensor upon exposure to a particular concentration of VOC vapor. Figure 4(b) presents the corresponding amplification factors of five VOCs. It is readily apparent that the HFBI coating improved the sensitivity of the FBAR sensor and that polar VOCs were adsorbed more strongly than nonpolar VOCs. The sensing mechanism of the proposed sensor is based on the BET model of multilayer physisorption as illustrated in Fig. 4(c).

According to Eq. (2), the concentrations of hexane, tetrahydrofuran, acetone, ethanol, and methanol at the P/P_0 value of 0.7 are found to be 111656, 133333, 1740042, 40152, and 89222 ppm, respectively. The corresponding frequency shifts of the HFBI-coated FBAR are 0.186, 1.638, 1.160, 1.140, and 2.539 MHz, respectively. The noise of the proposed sensor is estimated to be 0.3 kHz. Therefore, the detection limits of the five VOCs are found to be 180.2, 24.4, 44.0, 10.6, and 10.5 ppm, respectively, as listed in Table I.

By fitting with the BET equation, the values of v_m and C for the five VOCs were determined as listed in Table I. As these parameters

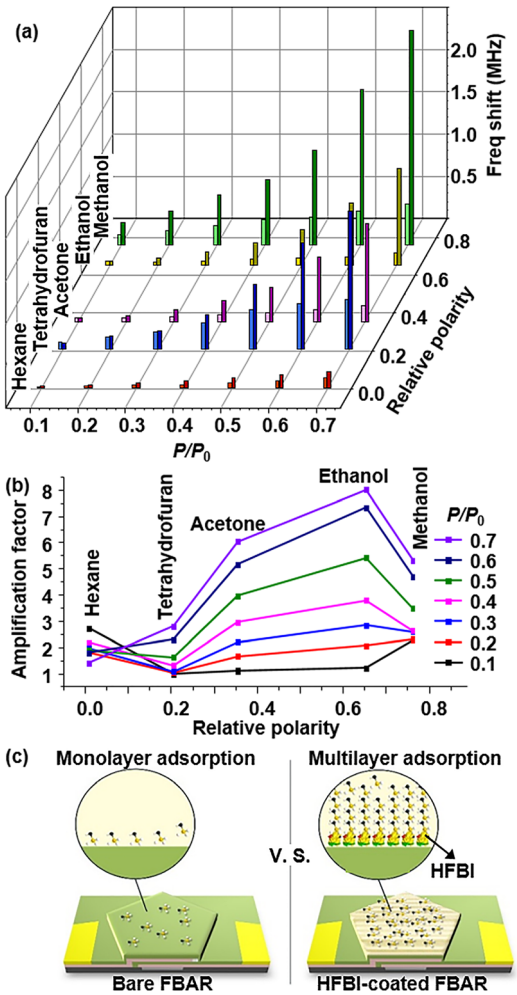

FIG. 4. (a) Frequency shifts and (b) amplification factors for various concentrations of five VOCs with different relative polarities. (c) Schematics of the monolayer adsorption of bare FBARs and the multilayer adsorption of HFBI-coated FBARs.

TABLE I. BET fitting results of v_m and C for the five VOCs.

VOC	Detection limits (ppm)	Relative polarity		HFBI-coated FBAR
Hexane	180.2 ± 10.8	0.009	v_m	65.1 ± 3.4
			C	3.8 ± 1.1
Tetrahydrofuran	24.4 ± 2.8	0.207	v_m	741.9 ± 120.1
			C	1.0 ± 0.4
Acetone	44.0 ± 6.2	0.355	v_m	676.0 ± 102.8
			C	0.5 ± 0.1
Ethanol	10.6 ± 0.6	0.654	v_m	614.5 ± 55.0
			C	0.6 ± 0.1
Methanol	10.5 ± 1.8	0.762	v_m	970.4 ± 67.8
			C	1.6 ± 0.4

are generally different for different VOCs, they can be used as fingerprints for gas discrimination. The v_m values for the HFBI-coated FBAR sensors were considerably larger than those for the bare FBAR sensors, which indicates that the HFBI surface can adsorb a greater amount of VOC molecules than that present in the single monolayer formed on the AlN surface of the bare FBAR sensor. Owing to its polarity, HFBI preferentially adsorbed polar VOCs. In other words, the number of VOC molecules adsorbed on the HFBI film increased with increasing VOC polarity.

In summary, this work demonstrated an HFBI-coated FBAR for the sensitive and polarity-sensitive sensing of VOCs. The measurement results show that the HFBI coating exerted a remarkable influence on the performance of the FBAR sensor and greatly enhanced its sensitivity by two- to eightfold. The adsorption isotherms were determined for the five VOCs. Fitting with the BET equation afforded the v_m and C values for the five VOCs, which can potentially be used as a fingerprint to discriminate different VOCs. The proposed HFBI-coated FBAR sensor possesses several advantages, such as the relatively simple coating method of droplet casting, the satisfactory stability of the HFBI coating, improved sensitivity, and polarity-sensitive sensing owing to the negatively charged nature of the HFBI film. This sensor holds great potential applications in biosensing owing to the multifunctional nature of HFBI.

The authors acknowledge the financial support of the Science and Technology Planning Project of Guangdong Province (No. 2016B010111003), the Science and Technology Development Plan Project of Jilin Province (Nos. 20180201024GX and 20190302062GX), and the National Key R&D Program of China (No. 2018YFB1801900). Zefang Wang acknowledges the support of the National Natural Science Foundation of China (No. 81601593).

REFERENCES

[1]A. H. Jalal, F. Alam, S. Roychoudhury, Y. Umasankar, N. Pala, and S. Bhansali, ACS Sens. **3**, 1246 (2018).
[2]J. E. Fitzgerald, E. T. H. Bui, N. M. Simon, and H. Fenniri, Trends Biotechnol. **35**, 33 (2017).
[3]K. Lee, D. H. Baek, J. Choi, and J. Kim, Sens. Actuators, B **264**, 249 (2018).
[4]A. D. Wilson, J. Forensic Sci. Criminol. **1**, 1 (2014).
[5]Y. Zhang, W. Yang, I. Simpson, X. Huang, J. Yu, Z. Huang, Z. Wang, Z. Zhang, D. Liu, Z. Huang, Y. Wang, C. Pei, M. Shao, D. R. Blake, J. Zheng, Z. Huang, and X. Wang, Environ. Pollut. **233**, 806 (2018).
[6]G. Lubes and M. Goodarzi, J. Pharm. Biomed. Anal. **147**, 313 (2018).
[7]M. Wang, L. Zeng, S. Lu, M. Shao, X. Liu, X. Yu, W. Chen, B. Yuan, Q. Zhang, M. Hu, and Z. Zhang, Anal. Methods **6**, 9424 (2014).
[8]X. Fan and I. M. White, Nat. Photonics **5**, 591 (2011).
[9]K. H. Kim, G. Bahl, W. Lee, J. Liu, M. Tomes, X. Fan, and T. Carmon, Light Sci. Appl. **2**, e110 (2013).
[10]K. Scholten, W. R. Collin, X. Fan, and E. T. Zellers, Nanoscale **7**, 9282 (2015).
[11]B. Szulczyński and J. Gębicki, Environments **4**, 21 (2017).
[12]S. E. Zohora, A. M. Khan, and N. Hundewale, Int. J. Soft Comput. Eng. **3**, 177 (2013).
[13]A. Mirzaei, S. G. Leonardi, and G. Neri, Ceram. Int. **42**, 15119 (2016).
[14]T. Allsop, R. Arif, R. Neal, K. Kalli, V. Kundrát, A. Rozhin, P. Culverhouse, and D. J. Webb, Light Sci. Appl. **5**, e16036 (2016).
[15]C. H. Park, V. Schroeder, B. J. Kim, and T. M. Swager, ACS Sens. **3**, 2432 (2018).
[16]S. Park, I. Yoon, S. Lee, H. Kim, J. W. Seo, Y. Chung, A. Unger, M. Kupnik, and H. J. Lee, Sens. Actuators, B **273**, 1556 (2018).
[17]M. Hernaez, C. R. Zamarreño, S. Melendi-Espina, L. R. Bird, A. G. Mayes, and F. J. Arregui, Sensors **17**, 155 (2017).
[18]S. H. Lee, Y. Jung, T. Kim, T. Kim, Y. Kim, and S. Jung, Proc. IEEE Sens. **1**, 1–4 (2015).
[19]M. L. Johnston, H. Edrees, I. Kymissis, and K. L. Shepard, in Proceedings of the IEEE International Conference on Micro Electro Mechanical Systems (2012), Vol. 846.
[20]M. Rinaldi, C. Zuniga, and G. Piazza, in Proceedings of the IEEE International Conference on Micro Electro Mechanical Systems (2011), Vol. 976.
[21]R. Gabl, E. Green, M. Schreiter, H. D. Feucht, H. Zeininger, R. Primig, D. Pitzer, G. Eckstein, and W. Wersing, Proc. IEEE Sens. **2**, 1184 (2003).
[22]Y. Lu, Y. Chang, N. Tang, H. Qu, J. Liu, W. Pang, H. Zhang, D. Zhang, and X. Duan, ACS Appl. Mater. Interfaces **7**, 17893 (2015).
[23]J. Hu, H. Qu, Y. Chang, W. Pang, Q. Zhang, J. Liu, and X. Duan, Sens. Actuators, B **274**, 419 (2018).
[24]Y. Chang, N. Tang, H. Qu, J. Liu, D. Zhang, H. Zhang, W. Pang, and X. Duan, Sci. Rep. **6**, 23970 (2016).
[25]G. Zeng, C. Wu, Y. Chang, C. Zhou, B. Chen, M. Zhang, J. Li, X. Duan, Q. Yang, and W. Pang, ACS Sens. **4**, 1524 (2019).
[26]X. Qiu, R. Tang, J. Zhu, H. Yu, J. Oiler, and Z. Wang, Proc. IEEE Sens., 1546–1549 (2010).
[27]J. Tao, Y. Wang, Y. Xiao, P. Yao, C. Chen, D. Zhang, W. Pang, H. Yang, D. Sun, Z. Wang, and J. Liu, Carbon **116**, 695 (2017).
[28]Z. Wang, Y. Wang, Y. Huang, S. Li, S. Feng, H. Xu, and M. Qiao, Carbon **48**, 2890 (2010).
[29]Z. Wang, M. Lienemann, M. Qiau, and M. B. Linder, Langmuir **26**, 8491 (2010).
[30]M. B. Linder, G. R. Szilvay, T. Nakari-Setälä, and M. E. Penttilä, FEMS Microbiol. Rev. **29**, 877 (2005).
[31]G. R. Szilvay, A. Paananen, K. Laurikainen, E. Vuorimaa, H. Lemmetyinen, J. Peltonen, and M. B. Linder, Biochemistry **46**, 2345 (2007).
[32]J. Hakanpää, A. Paananen, S. Askolin, T. Nakari-Setälä, T. Parkkinen, M. Penttilä, M. B. Linder, and J. Rouvinen, J. Biol. Chem. **279**, 534 (2004).
[33]M. B. Linder, Curr. Opin. Colloid Interface Sci. **14**, 356 (2009).
[34]R. Yamasaki, Y. Takatsuji, H. Asakawa, T. Fukuma, and T. Haruyama, ACS Nano **10**, 81 (2016).
[35]K. Scholtmeijer, J. G. H. Wessels, and H. A. B. Wösten, Appl. Microbiol. Biotechnol. **56**, 1 (2001).
[36]P. Laaksonen, M. Kainlauri, T. Laaksonen, A. Shchepetov, H. Jiang, J. Ahopelto, and M. B. Linder, Angew. Chem., Int. Ed. **49**, 4946 (2010).
[37]B. Della Ventura, I. Rea, A. Caliò, P. Giardina, A. M. Gravagnuolo, R. Funari, C. Altucci, R. Velotta, and L. De Stefano, Appl. Surf. Sci. **364**, 201 (2016).
[38]L. De Stefano, I. Rea, E. De Tommasi, I. Rendina, L. Rotiroti, M. Giocondo, S. Longobardi, A. Armenante, and P. Giardina, Eur. Phys. J. E **30**, 181 (2009).
[39]L. De Stefano, J. Nanophotonics **3**, 031985 (2009).
[40]L. De Stefano, I. Rea, P. Giardina, A. Armenante, and I. Rendina, Adv. Mater. **20**, 1529 (2008).
[41]L. De Stefano, I. Rea, A. Armenante, P. Giardina, M. Giocondo, and I. Rendina, Langmuir **23**, 7920 (2007).
[42]F. L. Tchuenbou-Magaia, I. T. Norton, and P. W. Cox, Food Hydrocolloids **23**, 1877 (2009).
[43]A. J. Green, K. A. Littlejohn, P. Hooley, and P. W. Cox, Curr. Opin. Colloid Interface Sci. **18**, 292 (2013).
[44]R. Bilewicz, J. Witomski, A. Van der Heyden, D. Tagu, B. Palin, and E. Rogalska, J. Phys. Chem. B **105**, 9772 (2001).
[45]J. Hakanpaa, Protein Sci. **15**, 2129 (2006).
[46]G. R. Szilvay, T. Nakari-Setälä, and M. B. Linder, Biochemistry **45**, 8590 (2006).
[47]W. Pang, H. Zhao, E. S. Kim, H. Zhang, H. Yu, and X. Hu, Lab Chip **12**, 29 (2012).
[48]H. Nguyen and S. A. El-Safty, J. Phys. Chem. C **115**, 8466 (2011).
[49]C. Zhang, S. Kaluvan, H. Zhang, G. Wang, and L. Zuo, Measurement **124**, 286 (2018).
[50]S. Brunauer, P. H. Emmett, and E. Teller, J. Am. Chem. Soc. **60**, 309 (1938).